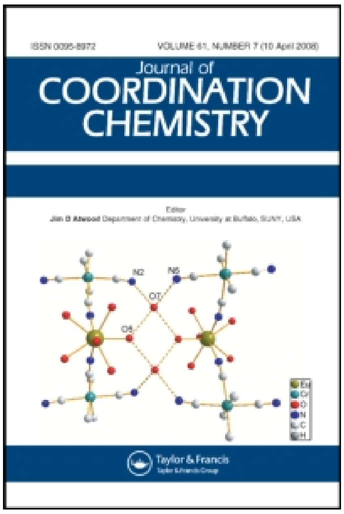

Journal of Coordination Chemistry

Publication details, including instructions for authors and subscription information:
http://www.informaworld.com/smpp/title~content=t713455674

Symmetric Ni(II) dithiocarbamates with bidentate phosphines ligands

Richard Pastorek[a]; Jiří Kameníček[a]; Boris Cvek[a]; Václav Slovák[b]; Marek Pavlíč[a]

[a] Department of Inorganic Chemistry, Palacký University, CZ-77147 Olomouc, Czech Republic [b] Department of Chemistry, Faculty of Science, University of Ostrava, CZ-70103 Ostrava, Czech Republic

To cite this Article Pastorek, Richard , Kameníček, Jiří , Cvek, Boris , Slovák, Václav and Pavlíč, Marek(2006) 'Symmetric Ni(II) dithiocarbamates with bidentate phosphines ligands', Journal of Coordination Chemistry, 59: 8, 911 — 919

To link to this Article: DOI: 10.1080/00958970500376187

URL: http://dx.doi.org/10.1080/00958970500376187

Journal of Coordination Chemistry
Vol. 59, No. 8, 20 May 2006, 911–919

Symmetric Ni(II) dithiocarbamates with bidentate phosphines ligands

RICHARD PASTOREK†, JIŘÍ KAMENÍČEK*†, BORIS CVEK†,
VÁCLAV SLOVÁK‡ and MAREK PAVLÍČEK†

†Department of Inorganic Chemistry, Palacký University, Křížkovského 10,
CZ-77147 Olomouc, Czech Republic
‡Department of Chemistry, Faculty of Science, University of Ostrava,
30 dubna 22, CZ-70103 Ostrava, Czech Republic

(*Received in final form 26 July 2006*)

Ni(II) mononuclear dithiocarbamate complexes with bidentate P,P ligands of composition $[Ni(R_2dtc)(P,P)]X$ {R = pentyl (pe), benzyl (bz); dtc = S_2CN^-; P,P = 1,2-bis(diphenylphosphino)ethane (dppe), 1,4-bis(diphenylphosphino)butane (dppb), 1,1′-bis(diphenylphosphino) ferrocene (dppf); X = ClO_4, Cl, Br, NCS} and binuclear complexes of composition $[Ni_2(\mu\text{-dpph})(R_2dtc)_2]X_2$ with a P,P-bridging ligand {P,P = 1,6-bis(diphenylphosphino)hexane (dpph); X = Cl, Br, NCS} have been synthesized. The complexes have been characterized by elemental and thermal analysis, IR, electronic and $^{31}P\{^1H\}$-NMR spectroscopy, magnetochemical and conductivity measurements. Single crystal X-ray analysis of $[Ni(pe_2dtc)(dppf)]ClO_4$ confirmed a distorted square planar coordination in the NiS_2P_2 chromophore. For selected samples, the catalysis of graphite oxidation was studied.

Keywords: Ni(II)-dithiocarbamate; Synthesis; X-ray structure; $^{31}P\{^1H\}$-NMR spectroscopy: Graphite oxidation

1. Introduction

There have been few studies of symmetrical Ni(II) dithiocarbamates with bidentate P,P-ligands. Only compounds involving dppe of composition $[Ni(R_2dtc)(dppe)]BPh_4 \cdot H_2O$ (R = phtalimidoethyl) [1], $[Ni(R_2dtc)(dppe)]ClO_4 \cdot CHCl_3$ (R = isopropyl) [2] and $[Ni(R_2dtc)(dppe)]BPh_4 \cdot H_2O$ (R = propyl) [3] have been reported. For these compounds, X-ray structure analyses confirmed a slightly distorted square arrangement around the central atom (NiS_2P_2 chromophore). Similar results were found for complex $[Ni(but_2dtc)(dppf)]X$ (X = ClO_4, I, but = butyl) [4]. McCleverty and Morrison [5] described the complex $[Ni(but_2dtc)(dppe)I]$ (NiS_2P_2I chromophore, coordination number five). In the present study, Ni(II)dipentyl (or dibenzyl) dithiocarbamate and

---

*Corresponding author. Email: dostalv@rupnw.upol.cz

Journal of Coordination Chemistry
ISSN 0095-8972 print: ISSN 1029-0389 online © 2006 Taylor & Francis
DOI: 10.1080/00958970500376187

dppb or dpph ligands were used as starting materials for the synthesis of new complexes with the aim of studying the influence of the type of dithiocarbamate and P,P-ligand on the structure of resulting compounds.

For selected complexes, thermal behaviour in connection with catalysis of graphite oxidation was studied. Graphite is an ideal model carbon material and results obtained for its oxidation in the presence of inorganic compounds as catalysts can be applied to other coal materials. Oxidative pyrolysis of these species with inorganic additives is widely applied in industry (for instance, influence of catalysts in the coal oxidation).

2. Experimental

2.1. *[Ni(R$_2$dtc)(P,P)]X (X=Cl, Br, ClO$_4$)*

A suspension of finely powdered [Ni(bz$_2$dtc)$_2$] [6] or [Ni(pe$_2$dtc)$_2$] [7] (1 mmol) in 20 cm^3 of methanol was mixed with $NiX_2 \cdot nH_2O$ (1 mmol) and the appropriate P,P-ligand (1 mmol) and stirred under reflux for 10 h. In the case of **VI**, a powder formed and this was filtered off and dried at room temperature. The product was dissolved in CHCl$_3$, filtered through active carbon and the complex obtained by addition of diethylether. For complexes **II**, **XIII** and **XIV**, crystals were obtained from solution after three days at room temperature (for **XIII**, **XI** it was possible to obtain single crystals appropriate for X-ray analysis). All products were filtered off and washed with diethylether. In the case of **I**, **III**, **IV**, **V**, **VII** and **VIII**, the solutions, after filtering through active carbon, were evaporated to small volume and an excess of water added; the complexes were isolated by freezing at −25°C. All products were washed with water and dried under an infrared lamp at 40°C. Yields: 39% (**I**), 20% (**II**), 42% (**III**), 46% (**IV**), 23% (**V**), 28% (**VI**), 45% (**VII**), 51% (**VIII**), 50% (**XIII**) and 57% (**XIV**).

2.2. *[Ni$_2$(μ-dpph)R$_2$dtc)$_2$X$_2$]*

A suspension of finely powdered [Ni(bz$_2$dtc)$_2$] or [Ni(pe$_2$dtc)$_2$] (1 mmol) in 20 cm^3 of methanol was mixed with $NiX_2 \cdot nH_2O$ (1 mmol) and dpph (1 mmol). After 10 h stirring, the solids that had separated out were collected by filtration, washed with water, methanol and diethylether, and dried under an infrared lamp at 40°C. Yields: 33% (**IX**), 48% (**X**), 38% (**XI**) and 60% (**XII**). Analytical data for the complexes are given in table 1; other characteristic data are summarized in table 2.

2.3. *Physical measurements*

Nickel content was determined by chelatometric titration with murexid as indicator [8]. Chlorine and bromine were determined by the Schöniger method [9]. C, H, N, S analyses were performed on aFisons EA 1108 instrument. Room temperature magnetic susceptibilities were measured by the Faraday method using Co[Hg(NCS)$_4$] as calibrant on a laboratory-designed instrument. Conductivities were measured with a WTW LF 330 meter at 25°C. Diffuse-reflectance electronic spectra (45,000–11,000 cm^{-1}) were measured on a Specord M 40 spectrophotometer and IR spectra (4000–400 cm^{-1}) on a Specord M 80 spectrophotometer using nujol mulls. Thermal analysis was performed

Table 1. Analytical data for the complexes.

Compound		Found (Calcd)%					
		M	Ni	C	H	N	X[a]
I	[Ni(pe$_2$dtc)(dppe)]ClO$_4$	789.0	7.1(7.4)	56.5(56.3)	6.3(5.9)	1.8(1.8)	4.0(4.5)
II	[Ni(bz$_2$dtc)(dppe)]ClO$_4$	829.0	7.1(7.1)	59.0(59.4)	5.1(4.6)	1.8(1.7)	3.8(4.3)
III	[Ni(bz$_2$dtc)(dppe)](NCS)	787.6	7.8(7.5)	63.6(64.0)	4.7(4.9)	3.5(3.6)	
IV	[Ni(bz$_2$dtc)(dppe)]Br $\cdot$ H$_2$O	827.4	7.1(7.1)	59.5(59.5)	4.8(4.9)	1.6(1.7)	10.2(9.7)
V	[Ni(pe$_2$dtc)(dppb)]Cl	753.1	8.0(7.8)	61.9(62.2)	7.2(6.7)	1.9(1.9)	5.0(4.7)
VI	[Ni(pe$_2$dtc)(dppb)]Br	797.5	7.1(7.4)	58.3(58.7)	6.7(6.3)	1.8(1.8)	10.3(10.0)
VII	[Ni(bz$_2$dtc)(dppb)]ClO$_4$ $\cdot$ 2H$_2$O	893.1	6.8(6.6)	57.6(57.8)	4.9(5.2)	1.6(1.6)	3.7(4.0)
VIII	[Ni(bz$_2$dtc)(dppb)]Br $\cdot$ H$_2$O	855.5	6.8(6.9)	59.9(60.4)	5.1(5.2)	1.7(1.6)	9.8(9.3)
IX	[Ni$_2$(μ-dpph)(pe$_2$dtc)$_2$Br$_2$]	1196.6	9.5(9.8)	51.8(52.2)	6.8(6.4)	2.3(2.3)	13.8(13.4)
X	[Ni$_2$(μ-dpph)(pe$_2$dtc)$_2$(NCS)$_2$]	1153.0	9.9(10.2)	56.0(56.3)	7.0(6.6)	4.8(4.9)	
XI	[Ni$_2$(μ-dpph)(bz$_2$dtc)$_2$Cl$_2$]	1187.6	9.4(9.9)	60.2(60.7)	5.0(5.1)	2.5(2.4)	6.4(6.0)
XII	[Ni$_2$(μ-dpph)(bz$_2$dtc)$_2$(NCS)$_2$]	1232.9	9.7(9.5)	59.9(60.4)	5.3(4.9)	4.6(4.5)	
XIII	[Ni(pe$_2$dtc)(dppf)]ClO$_4$	945.0	6.0(6.2)	56.9(57.2)	4.9(5.3)	1.5(1.5)	3.2(3.7)
XIV	[Ni(bz$_2$dtc)(dppf)]ClO$_4$	984.9	6.3(6.0)	59.5(59.8)	4.3(4.3)	1.4(1.4)	3.3(3.6)

[a] X = Cl, Br.

on a Exstar 6000 TG/DTA 6200 device (Seiko) between 20 and 1050°C, with a heating rate of 2.5°C min^{-1} and sample weights of 8.7–13.1 mg. ^{31}P{^{1}H}-NMR spectra were measured on a Bruker Avance 300 spectrometer, operating at frequency of 121.50 MHz, at 300 K. All samples were dissolved in CDCl$_3$; 85% H$_3$PO$_4$ was used as external reference. The thermoanalytic study of graphite catalytic oxidation was performed on a Netzsch STA 449C device with an α-Al$_2$O$_3$ crucible without standard; heating rate 10°C min^{-1}, sample weight 5.0 mg, dynamic atmosphere (air, 100 cm^3 min^{-1}). Samples were prepared by mixing graphite (0.6 g, diameter of particles less than 0.1 mm, ash residue max. 0.2%) and an acetone solution (2 cm^3) of the appropriate complex (**I**, **IX**, **XII**, **XIII**; [Ni] = 2.5 $\cdot$ 10^{-3} mol dm^{-3} and pure acetone – sample 0). All samples were homogenized by stirring and dried at room temperature for 24 h.

2.4. *Crystallography*

X-ray data collection was performed on a four-circle κ-axis Xcalibur$^{\mathrm{TM}}$2 diffractometer equipped with a Sapphire2 CCD detector, using Mo Kα radiation at 100 K. The CrysAlis program package (version 1.171.7, Oxford Diffraction) was used for data reduction. The structure was solved by direct methods using SHELXS-97 [10]; no absorption corrections were applied. The structure was refined anisotropically for all non-hydrogen atoms by full-matrix least-squares procedures using SHELXL-97 [11], while all hydrogen atoms were refined isotropically. Additional calculations were carried out using the PARST program [12]. Data concerning the structure analysis are given in tables 3–5.

3. Results and discussion

Mononuclear [Ni(R$_2$dtc)(P,P)]X complexes are diamagnetic and 1 : 1 electrolytes in acetone solution [13]. This is in agreement with a square planar NiS$_2$P$_2$

Table 2. Characteristic data for the complexes.*

							[°C]			
	Colour	λ_M[a]	ν(C···S)	ν(C···N)	IR [cm^{-1}][c]	$\lambda_{max} \times 10^3$ cm^{-1}	B	E_n	E_x	T_t
I	Light orange	153.4	1002w	1500w	ν_3 (ClO_4^-): 1086s; ν_4 (ClO_4^-): 622m	22.2; 30.0; 32.4	not studied			
II	Light orange	134.0	996m	1495m	ν_3 (ClO_4^-): 1080s; ν_4 (ClO_4^-): 620s	22.0; 29.3; 32.0	not studied			
III	Brown	137.7	996m	1500s	ν (C≡N): 2060s; ν (C–S): 744s	18.3; 30.6	43		183.9	92
IV	Brown	122.4	998m	1495s		18.2; 32.1	45			122
V	Orange	101.4	996m	1495m		20.6; 31.8	not studied			
VI	Orange	121.8	990w	1500w		21.0; 32.2		122;143	219;401	122[c];144[d]
VII	Orange	154.6	995w	1500m	ν_3 (ClO_4^-): 1088s; ν_4 (ClO_4^-): 620m	22.0; 31.5	not studied			
VIII	Dark brown	103.7	996w	1500m		18.0; 31.8	43	83.4	213.4	119
IX	Violet	2.2	1000w	1490m		19.0; 29.4	209	176.2	226.8	178
X	Red brown	1.5**	998w	1520m	ν(C≡N): 2088m; ν (C–S): 840m	20.8; 31.0	200	190		192
XI	Pink	N	1000m	1500m		19.5; 30.0	168.7	222.8	247.8	225
XII	Orange	4.7	984w	1498s	ν(C≡N): 2084s; ν (C–S): 835m	20.5 30.0	210	148.6		151
XIII	Red	149.2	996m	1500w	ν_3 (ClO_4^-): 1086s; ν_4 (ClO_4^-): 624m	19.6 31.5	not studied			
XIV	Red	142.0	995w	1505w	ν_3 (ClO_4^-): 1092s; ν_4 (ClO_4^-): 620m	19.2; 29.2	not studied			

*B: start of thermal decomposition; E_x: peak of exotherm; E_n: peak of endotherm; T_t: melting point.

[a] In acetone solution; **$[Ni^{2+}] = 10^{-3}$ mol dm^{-3}; S cm^2 mol^{-1}; N insoluble.

[b] Maxima in nujol.

[c] Amorphous form.

[d] Crystalline form.

Table 3. Crystal data and structure refinement details for [Ni(pe$_2$dtc)(dppf)]ClO$_4$.

Empirical formula	$C_{45}H_{50}ClFeNNiO_4P_2S_2$
Formula weight	944.93
Temperature (K)	100(2)
Wavelength (Å)	0.71073
Crystal system, space group	monoclinic, $C2/c$
Unit cell dimensions (Å, °)	$a = 20.143(4)$
	$b = 25.004(5)$
	$c = 17.539(4)$
	$\beta = 98.32(3)$
V (Å^3)	8741(3)
Z, Calculated density (Mg m^{-3})	8, 1.436
Absorption coefficient (mm^{-1})	1.036
$F(000)$	3936
Crystal size (mm)	0.40 × 0.40 × 0.10
θ range for data collection	2.81 to 32.11°
Index ranges	$-29 \le h \le 16$, $-36 \le k \le 36$, $-26 \le l \le 25$
Reflections collected/unique	44742/13977 [$R(\text{int}) = 0.0647$]
Completeness to $2\theta = 32.11°$	44.70%
Max. and min. transmission	0.9035 and 0.6820
Refinement method	Full-matrix least-squares on F^2
Data/restraints/parameters	13977/0/578
Goodness-of-fit on F^2	1.083
Final R indices [$I > 2\sigma(I)$]	$R_1 = 0.0620$, $wR_2 = 0.1400$
R indices (all data)	$R_1 = 0.1010$, $wR_2 = 0.1603$
Largest diff. peak and hole (e Å^{-3})	1.721 and −2.043

Table 4. Selected bond lengths (Å) and angles (°) for [Ni(pe$_2$dtc)(dppf)]ClO$_4$.

Ni(1)–P(1)	2.2014(9)	P(1)–Ni(1)–S(1)	91.00(3)
Ni(1)–S(1)	2.2025(10)	P(1)–Ni(1)–P(2)	101.16(3)
Ni(1)–P(2)	2.2180(9)	S(1)–Ni(1)–P(2)	167.22(3)
Ni(1)–S(2)	2.2297(9)	P(1)–Ni(1)–S(2)	166.78(3)
S(1)–C(1)	1.723(3)	S(1)–Ni(1)–S(2)	78.09(3)
S(2)–C(1)	1.715(3)	P(2)–Ni(1)–S(2)	90.32(3)
C(1)–N(1)	1.308(4)	C(1)–S(1)–Ni(1)	86.90(12)
		C(1)–S(2)–Ni(1)	86.23(11)

Table 5. Possible hydrogen bonds for [Ni(pe$_2$dtc)(dppf)]ClO$_4$.

D–H	D···A	H···A	D–H···A
C2–H2A	C2···S1	H2A···S1	C2–H2A···S1
0.96(27)	3.07(18)	2.75(2)	100.3(4)
1.080		2.735	97.84*
C3–H3A	C3···S1	H3A···S1	C3–H3A···S1
0.960(0.156)	3.44(11)	2.87(1)	119.7(5)
1.080		2.808	117.63*
C7–H7A	C7···S2	H7A···S2	C7–H7A···S2
0.99(4)	3.12(7)	2.47(2)	122.6(2)
1.080		2.424	120.79*
C51–H51	C51···S2	H51···S2	C51–H51···S2
0.90(4)	3.21(4)	2.91(2)	101.3(2)
1.080		2.884	97.72*
C32–H32	C32···O1(3)	H32···O1(3)	C32–H32···O1(3)
0.917(0.050)	3.17(2)	2.55(3)	125.0(1)
1.080		2.462	121.86*

*Values normalized following G.A. Jeffrey and L. Lewis, *Carbohydr. Res.*, **60**, 179 (1978); R. Taylor and O. Kennard, *Acta Cryst.*, **B39**, 133 (1983).

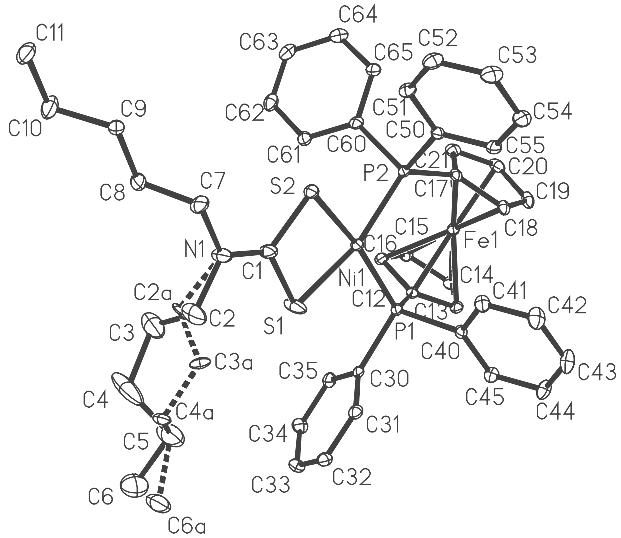

Figure 1. ORTEP drawing of [Ni(pe$_2$dtc)(dppf)]ClO$_4$ with the atom labelling scheme. Thermal ellipsoids are drawn at the 40% probability level; hydrogen atoms and the ClO$_4$ group are omitted for clarity.

chromophore [14]. Ionic nature of the X^- anion was supported by IR spectra; complexes with $X = ClO_4$ (**I**, **II**, **VII**, **XIII**, **XIV**) exhibit non-split maxima for ν_3 in the range 1080–1092 cm^{-1} and ν_4 between 620 and 624 cm^{-1} [15]. For **III** (X = NCS), ν(C≡N) of ionic NCS occurs at at 2060 and ν(C–S) at 744 cm^{-1} [16]. Square planar coordination is supported by electronic spectroscopy; bands in the 18,000–22,200 cm^{-1} region can be assigned to typical $^1A_{1g} \rightarrow {}^1B_{1g}$ transitions [17]. Bands over 30,000 cm^{-1} are probably connected with intra-ligand transitions in the S_2CN^- group [18].

The structure of [Ni(pe$_2$dtc)(dppf)]ClO$_4$ (see tables 3, 4, figure 1) confirmed these conclusions. Deviations of atoms from the ideal least-squares NiS$_2$P$_2$ plane are Ni(1), 0.004(1); S(1), 0.007(5); S(2), 0.002(2); P(1), 0.287(3); P(2), −0.216(2) Å. Significant π-bonding in C(1)–N(1), C(1)–S(1) and C(1)–S(2) is evident (table 4); bond lengths are shorter then published values for simple σ(C–N) and σ(C–S) bonds (1.47 and 1.81 Å) [19]. The ClO_4^- group lies out of the coordination sphere, corresponding with results given above. Best convergence was reached when chlorine was placed in two positions and three oxygen atoms O(2), O(3), O(4) from the ClO$_4$ group were calculated with occupancies of 0.5. Moreover, C(2), C(3), C(4) and C(6) carbon atoms from the pentyl group are disordered over two positions with occupancy factors of 0.75 and 0.25. A relatively large peak and hole in the final electron density map are situated near S1 (0.27 and 0.91 Å), attributed to series termination effects. Attempts to apply common absorption corrections (DIFABS, XABS2) were unsuccessful. The Ni–Ni distance (4.237 Å) is sufficiently long to preclude any interaction. Possible hydrogen bonds [12] in the lattice are listed in table 5.

The binuclear complexes **IX**–**XII** of [Ni$_2$(μ-dpph)(R$_2$dtc)$_2$X$_2$] type are also diamagnetic. Complexes **IX**, **X**, **XI** are non-electrolytes; the conductivity of **XI** was not estimated due to solubility problems. Compounds with NCS (**X**, **XII**) exhibit the ν(C≡N) IR vibrations at 2085 cm^{-1} and ν(C–S) at 840 cm^{-1}; this can be explained [16, 20] by coordination of NCS to nickel via nitrogen. From the results it is concluded

Table 6. $^{31}P\{^1H\}$-NMR data for the complexes[a].

Compound	δ (ppm)	$\Delta_{complex}–\delta_{ligand}$ (ppm)
dppe	−11.86(singlet)	
dppb	−15.43(singlet)	
dpph	−15.42(singlet)	
dppf	−16.55(singlet)	
$[Ni(pe_2dtc)(dppe)]ClO_4$	62.13(singlet)	73.99
$[Ni(bz_2dtc)(dppe)]ClO_4$	62.44(singlet)	74.3
$[Ni(bz_2dtc)(dppe)](NCS)$	62.46(singlet)	74.32
$[Ni(bz_2dtc)(dppe)]Br \cdot H_2O$	62.11(singlet)	73.97
$[Ni(pe_2dtc)(dppb)]Cl$	28.57(singlet)	44
$[Ni(pe_2dtc)(dppb)]Br$	29.07(singlet)	44.5
$[Ni(bz_2dtc)(dppb)]ClO_4 \cdot 2H_2O$	29.20(singlet)	44.63
$[Ni(bz_2dtc)(dppb)]Br \cdot H_2O$	28.18(singlet)	43.61
$[Ni_2(\mu\text{-dpph})(pe_2dtc)_2Br_2]$	19.54(singlet)	34.96
$[Ni_2(\mu\text{-dpph})(pe_2dtc)_2(NCS)_2]$	19.55(singlet)	34.97
$[Ni_2(\mu\text{-dpph})(bz_2dtc)_2Cl_2]$	16.95(singlet)	32.37
$[Ni_2(\mu\text{-dpph})(bz_2dtc)_2(NCS)_2]$	19.52(singlet)	34.94
$[Ni(pe_2dtc)(dppf)]ClO_4$	32.21(singlet)	48.76
$[Ni(bz_2dtc)(dppf)]ClO_4$	32.29(singlet)	48.84

[a] In $CDCl_3$ solution.

that nickel is in a nearly square planar arrangement and dpph is coordinated as a bidentate. Similar results were obtained recently [21] for $[Ni_2(\mu\text{-dpph})(hmidtc)_2Br_2]$ (hmidtc = hexamethyleniminedithiocarbamate). Assumption of square planar coordination is supported by electronic spectroscopy; maxima in the 19,000–20,800 cm^{-1} region can be assigned to typical $^1A_{1g} \rightarrow {}^1B_{1g}$ transitions [17] and bands over 30,000 cm^{-1} are probably again connected with intra-ligand transitions in the S_2CN^- group [18]. IR-spectra were not studied in detail; all complexes exhibit typical dithiocarbamate vibrations, $\nu(C\cdots N)$ between 990 and 1002 cm^{-1} and $\nu(C\cdots S)$ in the interval 1490–1520 cm^{-1} [18].

^{31}P-NMR spectra of all complexes exhibit only one signal, indicating that both phosphorus atoms in the P,P ligand are magnetically equivalent (table 6). Significant change in chemical shift in comparison to free ligands is caused by coordination to nickel. Complexes **I**–**IV** with coordinated dppe are characterized by a singlet (62.11–62.46 ppm), complexes **V**–**VIII** with dppb (28.18–29.20 ppm) and complexes **XIII**–**XIV** with dppf (32.21–32.29 ppm). Spectra of binuclear complexes with bridging dpph ligand **IX**–**XII** exhibit singlets in the range 16.95–19.55 ppm. Due to coordination, a shift to the higher values was observed in the order dpph < dppb < dppf < dppe.

Thermoanalysis (see table 2) showed that the binuclear complexes **IX**–**XII** are thermally more stable (start of decomposition between 168.7 and 210°C), whereas mononuclear complexes are less so (45°C). Endothermic effects in the range 148–223°C are connected with melting, as confirmed by melting point determinations. Most interesting is the thermal decomposition of **VI**. DTA curves exhibit two small endo-effects at 122 (amorphous phase) and 143.5°C (crystalline form). Thus the sample probably consists of both. The small exo-effect observed at 219°C is connected with a small mass increase on the TG curve. This can be explained by the insertion of oxygen into the Ni–P bond as recently described in the literature [22]. However, the insertion of oxygen is followed by thermal decomposition (exo-effect at 401°C).

Table 7. Characteristic temperatures (°C) and kinetic parameters of graphite oxidation by selected complexes[a].

Complex	T_p	T_m	T_k	n	A (s^{-1})	E (kJ mol^{-1})
0	763	818	844	0.8	$2.99 \cdot 10^{10}$	259
I	783	845	883	0.9	$3.06 \cdot 10^{9}$	250
IX	769	834	876	0.9	$1.75 \cdot 10^{8}$	222
XII	722	804	862	1.1	$3.46 \cdot 10^{6}$	190
XIII	722	801	851	1.0	$6.09 \cdot 10^{6}$	190

[a] T_p: start of oxidation; n: reaction order; T_m: rate maximum; A: frequency factor; T_k: end of oxidation; E: activation energy.

Similar effects were observed for **III** (184°C), **VIII** (213°C), **IX** (227°C) and **XI** (248°C); the small endo-effect (83°C) for **VIII** is connected with water elimination. Compounds with perchlorate were not studied from safety reasons.

From DTG curves and characteristic temperatures (table 7) is apparent that the influence of samples on graphite oxidation is different. For **I** and **IX**, the temperature at the start of oxidation is higher in comparison to pure graphite. Similar effects are noted for T_m and T_k. In contrast, complexes **XII** and **XIII** lowered T_p; however, T_k is still higher than for pure graphite. All kinetic parameters were calculated for a one-step mechanism of oxidation [23] by non-linear regression methods. Differences in reaction order n are very small; all samples (especially **XII**, **XII**) exhibit lower E_a values than that of pure graphite. The complexes exert only a small influence on graphite oxidation. With **I** and **IX** graphite oxidation proceeds slowly, but activation energy is smaller; therefore classical inhibition can not be assumed. Both **XII** and **XIII** caused a significant decrease of T_p and E_a values.

Supplementary data

Crystallographic data are deposited in the Cambridge Crystallographic Data Centre, No. CCDC 274142.

Acknowledgements

The authors would like to thank the Granting Agency of Czech Republic (grant No. MSM 6198959218) for support of this work. We also thank Zdeněk Šindelář for magnetochemical measurements and Michal Maloň for NMR spectra.

References

[1] V. Venkatachalam, K. Ramalingam, G. Bocelli, A. Cantoni. *Inorg. Chim. Acta*, **257**, 49 (1997).
[2] V. Venkatachalam, K. Ramalingam, C.W. Thomas, Luo Bao-Seng. *Polyhedron*, **15**, 1295 (1996).
[3] B.A. Prakasam, K. Ramalingam, M. Saravanan, G. Bocelli, A. Cantoni. *Polyhedron*, **23**, 77 (2004).
[4] R. Pastorek, J. Kameníček, M. Pavlíček, J. Husárek, Z. Šindelář, Z. Žák. *J. Coord. Chem.*, **55**, 1301 (2002).
[5] J.A. McCleverty, N.J. Morrison. *J. Chem. Soc., Dalton Trans.*, 541 (1976).
[6] Gmelins Handbuch der Anorganischen Chemie, Nickel, Teil C, Lief. 2, p. 996, Verlag Chemie, Weinheim (1969).
[7] R. Pastorek, J. Kameníček, B. Cvek, M. Pavlíček, Z. Šindelář, Z. Žák. *J. Coord. Chem.*, **56**, 1123 (2003).
[8] R. Přibil. *Komplexometrické titrace*, p. 22, SNTL, Praha (1955).
[9] M. Jureček. *Organická analýza II*, p. 140, ČSAV, Praha (1957).

[10] G.M. Sheldrick. *Acta Crystallogr.*, **A46**, 467 (1990).

[11] G.M. Sheldrick. *SHELXL-97, Program for Crystal Structure Refinement*, University of Göttingen, Germany (1997).

[12] M. Nardelli. *J. Appl. Cryst.*, **28**, 659 (1995).

[13] W.J. Geary. *Coord. Chem. Rev.*, **7**, 81 (1971).

[14] A.B. Nejding. *Magnetochimija komplexnych sojedinenij perechodnych metallov*, p. 165, Mir, Moskva (1970).

[15] R.P. Scholer, E.A. Merbach. *Inorg. Chim. Acta*, **15**, 15 (1975).

[16] N.B. Colthup, L.H. Daly, S.E. Wiberley. *Introduction to Infrared and Raman Spectroscopy*, p. 204, Academic Press, New York (1964).

[17] A.B.P. Lever. *Inorganic Electronic Spectroscopy*, p. 534, Elsevier, Amsterdam (1984).

[18] C.A. Tsipis, D.P. Kessissoglou, G.A. Katsoulos. *Chim. Chron.*, *New Series*, **14**, 195 (1985).

[19] D.R. Lide (Ed.). *Handbook of Chemistry and Physics*, 73rd Edn, CRC Press, Boca Ralton, FL (1992).

[20] I.E. Černikova, I.A. Chartonik, D.S. Umrejko, A.B. Kavrikov, V.I. Afanov. *Koord. Chim.*, **15**, 1695 (1989).

[21] R. Pastorek, J. Kameníček, J. Husárek, M. Pavlíček, Z. Šindelář, Z. Žák. *Polish J. Chem.*, **77**, 805 (2003).

[22] F. Březina, E. Benátská. *J. Thermal Anal.*, **22**, 75 (1981).

[23] V. Slovák. *Thermochim. Acta*, **372**, 175 (2001).